Downfolding: effective model construction from first principles simulation

Huihuo Zheng*
Argonne Leadership Computing Facility, Argonne National Laboratory,
9700 Cass Avenue, Lemont, 60439, Illinois, USA
(Dated: July 23, 2017)

In this note, I will summarize the basic formalism of downfolding, with demonstration of several systems including molecules and solids. The results are based on Chapter 4 and Chapter 6 of my PhD dissertation[1].

I. INTRODUCTION

Physicists usually like to have an intuitive understanding of physical phenomena using simplified models. These models are expected to capture the most relevant physical degrees of freedom related to the observed phenomena. For example, at high temperature and low density when quantum effect is not significant, the ideal gas model can successfully capture the statistical properties of 10^{23} H_2 molecules in a box, without any detailed knowledge of the fundamental constituent of H_2. This approach is valid when we are interested in phenomena at certain energy scale (or length scale), while the degrees of freedom at other length scales which are not dynamically excited simply renormalize the dynamics of the low energy degrees of freedom.

This concept/principle has been widely employed in condensed matter physics. For example, in the past decades, there are a lot of studies on describing complex systems (high Tc Cuprate and many other transition metal oxides) using models such as Hubbard model[2], t-J model[3], etc. However, very few studies have addressed the effectiveness of those models in describing the real complex systems. In complex systems such as high Tc cuprates, it is unclear to what extent can these models describe the reality[4]. Generally, in strongly correlated systems, the macroscopic phenomena are strongly dependent on material-specific properties, motivating the need to determine the effective Hamiltonians that can capture all necessary details.

On the other hand, the reliable simulation of systems for which the large-scale physics is not well-approximated by a non-interacting model, is a major challenge in physics, chemistry, and materials science. These systems appear to require a multi-scale approach in which the effective interactions between electrons at a small distance scale are determined, which then leads to a coarse-grained description of emergent correlated physics. This reduction of the Hilbert space is often known as "downfolding".

A schematic of "downfolding" is depicted in Fig. 1. The full Hamiltonian H is defined in the space of active (partially occupied), core (mostly occupied) and virtual (mostly unoccupied) orbitals. These orbitals have been arranged according to their energy (E) in the figure. The objective is to map the physics of the original system to that of the effective one, defined only in the active space, with Hamiltonian $\tilde{H}$. Once an effective model Hamiltonian in the reduced Hilbert space is obtained, it can be used to perform a calculation on a larger system using techniques designed for lattice models[5–18]. This multi-step modeling procedure is needed since the *ab initio* calculations for a given system size are, in general, computationally more expensive than the equivalent lattice calculations. Large sizes are crucial to study finite size effects, and in turn theoretically establish the presence of a phase. In addition, excited states and dynamical correlation functions have traditionally been difficult in *ab initio* approaches, but have seen progress for lattice model methods[19–21].

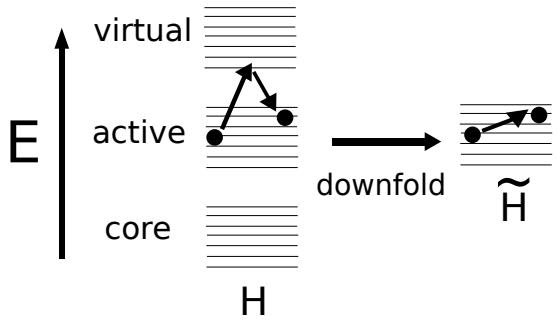

FIG. 1. Schematic for downfolding. The full Hamiltonian H is defined in the space of active (partially occupied), core (mostly occupied) and virtual (mostly unoccupied) orbitals. These orbitals have been arranged according to their energy (E) in the figure. The objective is to map the physics of the original system to that of the effective one, defined only in the active space, with Hamiltonian $\tilde{H}$.

One can loosely categorize downfolding techniques into two strategies. The first strategy is based on performing *ab initio* calculations and then matching them state by state to the effective model. Alternately, some approaches employ a model for the screening of Coulomb interactions, for which the *ab initio* single particle wavefunctions provide the relevant inputs. Techniques that fall into this class include the constrained density functional theory[22,23], the constrained random phase approximation (cRPA)[24], fitting spin models to energies[25,26], and fitting reduced density matrices of quantum Monte Carlo (QMC) calculations to that of model Hamiltonian[27]. The second class is based on Löwdin downfolding[28–30] and canonical transformation theory[31–35], which involves a sequence of unitary transformations on the bare Hamiltonian, chosen in a way that minimize the size of the matrix elements connecting the relevant low energy (valence) space to the high energy one.

Downfolding by fitting has the advantage that it is conceptually straightforward to perform, although it demands an

a priori parameterization of the effective Hamiltonian. The methods have been applied to complex bulk systems[36–41], but it is only recently that their accuracy is being rigorously checked[42]. On the other hand, canonical transformations do not need such parameterizations and can discover the relevant terms in an automated way. However, their application to complex materials remains to be carried out and tested.

In this note, we demonstrate three downfolding methods that use data from *ab initio* QMC techniques to derive an effective coarse-grained Hamiltonian.

(1) Eigenstate *ab initio* density matrix downfolding (E-AIDMD): we optimize model parameters to match the density matrix and energy spectrum of the model Hamiltonian to that of the *ab initio* system. In this method, we build a one to one correspondence between the states of the model Hamiltonian and that of the *ab initio* Hamiltonian. To accomplish this, we need to solve both the model Hamiltonian and the *ab initio* Hamiltonian. Generally, we need to find a cheaper way to solve model Hamiltonian such that we can efficiently solve it multiple times for different parameters in order to find the optimized set of parameters that can match the *ab initio* system.

(2) Non-eigenstate *ab initio* density matrix downfolding (NE-AIDMD): this is based on the fact that, once a model Hamiltonian is assumed, the energy expectation of a certain state is directly related to the reduced density matrix on that state. Thus, each state imposes a constraint for the model parameters. We can choose several low lying states (not necessary to be the eigenstates of the system), and form a linear least fitting problem for the model parameters. Solving the linear least problem will determine the value of the parameters. Meanwhile, analyzing the residue of the fitting also give us a quantitative estimate of how good the model is.

(3) Non-eigenstate *ab initio* EKT (extended Koopmans' theorem) matrix downfolding (EKT-AIDMD): this is similar to the NE-AIDMD, except that now we use the EKT matrices $\mathcal{V}$ and $\mathcal{C}$ [see Eqs. (**??**) and (**??**)] instead of energy. Compared with NE-AIDMD, we have much more information (all the matrix elements of $\mathcal{V}$ and $\mathcal{C}$) in EKT-AIDMD to impose constraints on the parameters, instead of just the energy expectation for a particular state. Through the quality of the linear least fit, one can also assess the quality of the low energy model in describing the low energy physics of the system.

In the following section, we will first provide detailed formulation of the three downfolding methods. We will then use the three methods to study the most simple "many-body" system, H_2 molecule, to demonstrate the idea/procedure of the downfolding process. We will then apply these methods to solids, in particular, the one-dimensional hydrogen chain and graphene.

II. DOWNFOLDING PROCEDURES

A. Eigenstate AIDMD method (E-AIDMD)

In the first method, schematically depicted in Fig. 2(a), eigenstates from an *ab initio* calculation are used to match density matrices and energies of the corresponding model. The parameters of the model Hamiltonian are obtained by minimizing a cost function that is a linear combination of the energy and density matrix errors,

$$\mathcal{R} \equiv \sum_s (E_s^a - E_s^m)^2 + f \sum_s \sum_{i,j,k,l} (\langle c_i^\dagger c_j^\dagger c_l c_k \rangle_s^a - \langle c_i^\dagger c_j^\dagger c_l c_k \rangle_s^m)^2 \,. \tag{1}$$

where the subscript s is an eigenstate index, i, j, k, l are orbital indices and the superscripts a and m refer to *ab initio* and model calculations respectively. Here, we only include the two-body reduced density matrix, but not the one-body reduce density matrix, since the latter is completely determined by the former. There is no definite prescription for choosing the weight f; a good heuristic is to choose a value that gives roughly the same size of errors for the two terms that enter the cost function. The cost minimization is performed with the Nelder Mead simplex algorithm.

This method is limited by the number of available eigenstates and the accuracy of true estimators. This method requires accurate model solvers. Currently, it is only applicable to models that are exactly solvable.

B. Non-eigenstate AIDMD method (NE-AIDMD)

Consider a set of *ab initio* energy averages $\tilde{E}_s$, i.e. expectation values of the Hamiltonian, and corresponding 1- and 2-RDMs $\langle c_i^\dagger c_j \rangle_s$, $\langle c_i^\dagger c_j^\dagger c_l c_k \rangle_s$ for arbitrary low-energy states characterized by index s. Assume a model 2-body

Hamiltonian with effective parameters t_{ij} (1-body part) and $V_{i,j,k,l}$ (2-body part) along with a constant term C; the total number of parameters being N_p. Then for each state s, we have the equation,

$$\tilde{E}_s \equiv \langle H \rangle_s = C + \sum_{ij} t_{ij} \langle c_i^\dagger c_j \rangle + \sum_{ijkl} V_{ijkl} \langle c_i^\dagger c_j^\dagger c_l c_k \rangle \,, \tag{2}$$

where we have made the assumption that the chosen set of operators corresponding to single particle wavefunctions or orbitals, explain all energy differences seen in the *ab initio* data. The constant C is from energetic contributions of all other orbitals which are not part of the chosen set.

We then perform calculations for M low-energy states which are not necessarily eigenstates. These states are not arbitrary in the sense that they have similar descriptions of the core and virtual spaces. Each state satisfies the criteria (1) its energy average does not lie outside the energy window of interest and (2) the trace of its 1-RDM matches the electron number expected in the effective Hamiltonian.

The objective of choosing a sufficiently big set of states is to explore parts of the low-energy Hilbert space that show variations in the RDM elements. Since the same parameters describe all M states, they must satisfy the linear set of equations,

$$\begin{pmatrix} \tilde{E}_1 \\ \tilde{E}_2 \\ \tilde{E}_3 \\ ... \\ ... \\ ... \\ ... \\ \tilde{E}_M \end{pmatrix} = \begin{pmatrix} 1 & \langle c_i^\dagger c_j \rangle_1 & .. & \langle c_i^\dagger c_j^\dagger c_l c_k \rangle_1 & .. \\ 1 & \langle c_i^\dagger c_j \rangle_2 & .. & \langle c_i^\dagger c_j^\dagger c_l c_k \rangle_2 & .. \\ 1 & \langle c_i^\dagger c_j \rangle_3 & .. & \langle c_i^\dagger c_j^\dagger c_l c_k \rangle_3 & .. \\ 1 & \langle c_i^\dagger c_j \rangle_4 & .. & \langle c_i^\dagger c_j^\dagger c_l c_k \rangle_4 & .. \\ 1 & .... & .. & .. & .. \\ 1 & .... & .. & .. & .. \\ 1 & \langle c_i^\dagger c_j \rangle_M & .. & \langle c_i^\dagger c_j^\dagger c_l c_k \rangle_M & .. \end{pmatrix} \begin{pmatrix} C \\ t_{ij} \\ .. \\ V_{ijkl} \\ .. \end{pmatrix} \tag{3}$$

which is compactly written as,

$$\mathbf{E} = A\mathbf{x} \,, \tag{4}$$

where $\mathbf{E} \equiv (\tilde{E}_1, \tilde{E}_2, ...\tilde{E}_M)^T$ is the M dimensional vector of energies, A is the $M \times N_p$ matrix composed of density matrix elements and $\mathbf{x} \equiv (C, t_{ij}....V_{ijkl}...)^T$ is a N_p dimensional vector of parameters. This problem is over-determined for $M > N_p$, which is the regime we expect to work in.

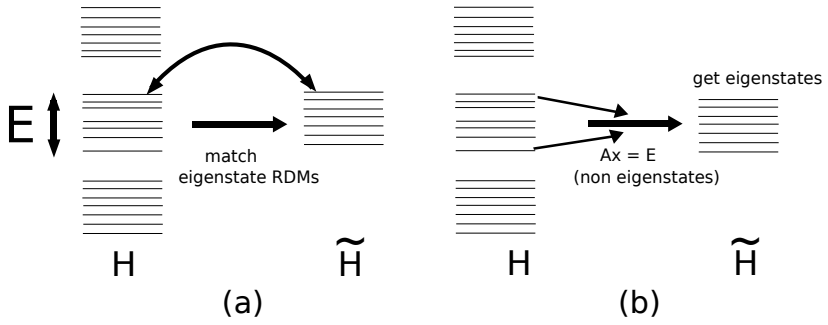

FIG. 2. Schematic of *ab initio* density matrix downfolding (AIDMD) methods employed for determining the effective Hamiltonian parameters. (a) In the eigenstate (E)-AIDMD, the reduced density matrices and energies of eigenstates of the model are matched to the *ab initio* counterparts. (b) The non-eigenstate (N)-AIDMD method uses RDMs and energies of arbitrary low-energy states to construct a matrix of relevant density matrices and performs a least square fit to determine the optimal parameters.

In the case of any imperfection in the model, which is the most common case, the equality will not hold exactly and one must then instead minimize the norm of the error, $\mathcal{R}$:

$$\mathcal{R} \equiv ||A\mathbf{x} - \mathbf{E}||^{\mathbf{2}} \,. \tag{5}$$

This cost function can be minimized in a single step by using the method of least squares, employing the singular value decomposition of matrix A. This matrix also encodes exact (or near-exact) linear dependences. Thus, the quality of the fit is directly judged by assessing (1) the singular values of the A matrix and (2) the value of the cost function

itself i.e. the deviations of the input and fitted energies. We will refer to this as the non eigenstate NE-AIDMD method throughout the rest of the paper. This idea is schematically depicted in Fig. 2(b).

The matrix A gives a very natural basis for understanding renormalization effects. For example, consider a set of wavefunctions that show that the correlator $\langle n_i n_j \rangle$ does not change significantly. This would lead to the corresponding column of matrix A being identical (up to a scale factor) to the first column of 1's. Physically, this would correspond to the coupling constant V_{ijji} being irrelevant for the low-energy physics; it can take any value including zero and can be absorbed into the constant shift term. This could also alternatively mean that the input data is correlated and does not provide enough information about V_{ijji}, so care must be taken in constructing the set of wavefunctions.

In summary, the N-AIDMD method performs the following operation. The 1- and 2-RDMs and energy expectation values of many non-eigenstate correlated states are calculated. Then, given an effective Hamiltonian parameterization, linear equations (4) are constructed and solved. Standard model fitting principles apply, and we can evaluate the goodness of fit to determine whether a given effective Hamiltonian can sufficiently describe the data.

III. APPLICATION OF DOWNFOLDING METHODS TO SOLID SYSTEMS

In this section, we apply our downfolding methods to solid systems. We will mainly consider three systems here, one dimensional hydrogen chain, graphene, and hydrogen honeycomb systems.

A. One dimensional hydrogen chain (E-AIDMD)

Let us consider the following single band model Hamiltonian,

$$H = \sum_i \left\{ -t[c^\dagger_{i\sigma} c_{i+1\sigma} + h.c.] + V n_i n_{i+1} + U n_{i\uparrow} n_{i\downarrow} + J \boldsymbol{\sigma}_i \cdot \boldsymbol{\sigma}_{i+1} \right\} + C \,. \tag{6}$$

Here, c_i's are Wannier orbitals generated from Kohn-Sham orbitals. We consider the case where the interatomic distance is relatively large, such that the system could be well described by a single band. We start from the 4-site hydrogen chain with bond length equals to 2Åwith periodic boundary condition. We construct the Wannier orbitals by a unitary transformation of the four lowest energy Kohn-Sham states obtained from DFT/PBE calculation (2 occupied and 2 unoccupied). Fig. 3 shows the selected Kohn-Sham orbitals and constructed Wannier orbitals.

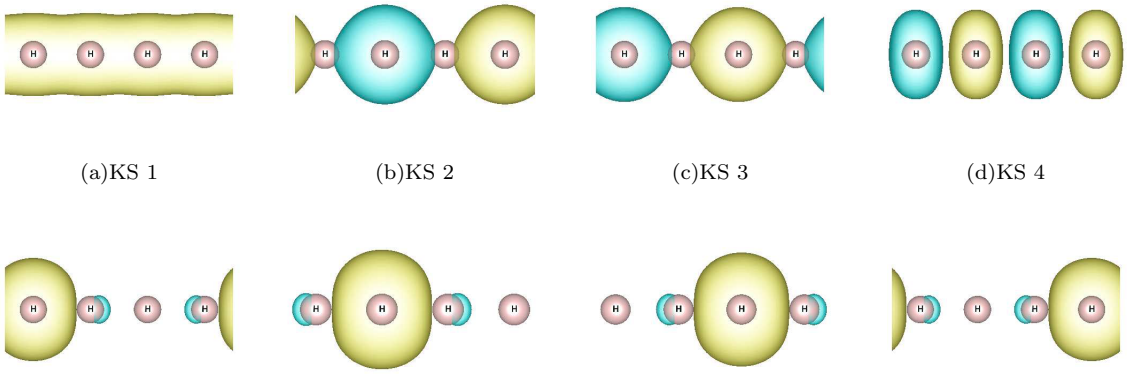

(a)KS 1 (b)KS 2 (c)KS 3 (d)KS 4

(e)Wannier 1 (f)Wannier 2 (g)Wannier 3 (h)Wannier 4

FIG. 3. Kohn-Sham orbitals (upper panel) from DFT calculations with PBE exchange-exchange correlation functional, and Wannier orbitals (lower panel) constructed through a unitary transformation of Kohn-Sham orbitals.

We will use the mentioned E-AIDMD method to downfold the ab initio system into the model Hamiltonian in Eq. (6) by matching the single-body energy spectra and the 1-body and 2-body reduced density matrices. The model Hamiltonian is solved by exact diagonization, whereas the *ab initio* system is solved using diffusion Monte Carlo method with single Slater-Jastrow trial wave functions.

In our calculations, we used energies and RDMs of the following three states:

$$S = 0: \quad E = -2047.8(6)\text{mHa}; \tag{7a}$$
$$S = 1: \quad E = -2038.9(5)\text{mHa}; \tag{7b}$$
$$S = 2: \quad E = -1957.8(3)\text{mHa}. \tag{7c}$$

where S is the total angular moment of such the four-site hydrogen chain. In order to understand the relative importance of various two-body terms: (a) the onsite Hubbard interaction – $\hat{U}$; (b) nearest neighbor Coulomb interaction – $\hat{V}$; (c) nearest neighbor exchange – $\hat{J}$, we compare the parameters obtained when downfolding the system to the following three different models with different two-body interactions,

(a) **UVJ** model: onsite Hubbard interaction(U), nearest neighbor Coulomb (V) and exchange (J);

(b) **UV** model: onsite Hubbard interaction(U), nearest neighbor Coulomb (V); J is set to zero.

(c) **U** model: onsite Hubbard interaction(U). V and J are set to zero.

The quality of downfolding is measured by the relative error of the two-body reduced density matrices, and the error of the eigen energies of the three states.

$$R_{err} = \sqrt{\frac{\sum_{i,j,k,l}(M_{ijkl}^{\text{ab initio}} - M_{ijkl}^{\text{model}})^2}{\sum_{i,j,k,l}(M_{ijkl}^{\text{ab initio}})^2}}, \quad \Delta E = \sqrt{\sum_i |E_i^{\text{ab initio}} - E_i^{\text{model}}|^2}\,. \tag{8}$$

The resulting effective parameters are showed in Table. I. We see that all the three models can match the *ab initio* data accurately. U model has relatively larger error in energy, but it is still comparable to the stochastic error from QMC ($0.3 \sim 0.5$ mHa).

TABLE I. Parameters of effective Hamiltonian [mHa], and error of RDMs and energies [mHa].

Model	t	U	V	J	err(RDM)	err(energy)
UVJ	23.68	34.58	0.03	-3.11	0.25%	10^{-13}
UV	32.76	130.63	65.31	/	0.75%	10^{-13}
U	37.45	114.62	/	/	0.26%	1.8

1. *Transferability of the model parameters to larger systems*

In order to verify the transferability of the parameters for larger systems. We study longer chains (6-site, 8-site and 10-site) with the same interatomic distance (2Å), and examine whether our parameters obtained from the 4-sites hydrogen chain is able to match the low energy physics of longer chains. We therefore, solve the model Hamiltonian with the parameters from Table. I, and examine the errors of the RDMs of S=0 and S=1 states. The results are shown in Fig. 4. As we can see, the error of the RDMs is around 10%, indicating that the downfolding parameters from a smaller system is transferable to larger systems. Therefore, at $d = 2$Å, the hydrogen chain can be described by the extended Hubbard model (6) very well.

B. Graphene and hydrogen lattice (NE-AIDMD)

In this subsection, we will downfold graphene and hydrgoen (with the same lattice constant $a = 2.46$Å) into the following effective Hubbard model,

$$\hat{H} = C + t\sum_{\langle i,j\rangle} c_{i,\sigma}^\dagger c_{j,\sigma} + \text{h.c.} + U\sum_i n_{i,\uparrow}n_{i,\downarrow}\,. \tag{9}$$

where we only include π orbitals in the effective model of graphene, and s orbitals in the effective model of hydrogen. $c_i's$ are Wannier orbitals constructed from Kohn-Sham orbitals, shown in Fig. 5.

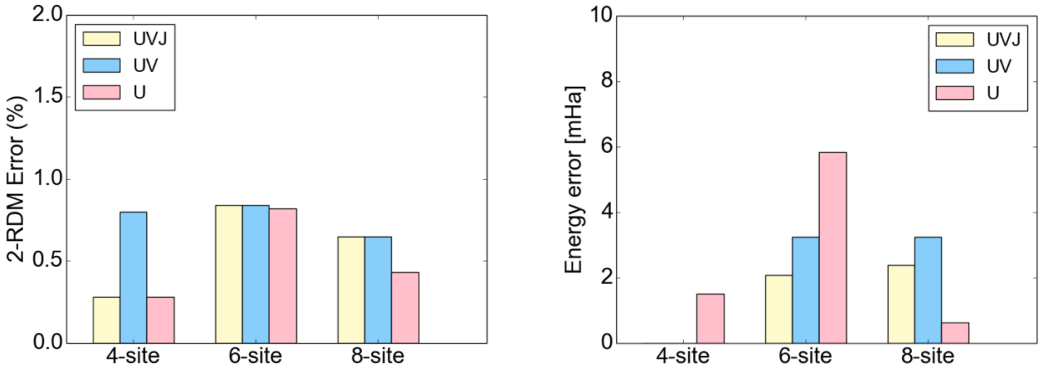

(a) (b)

FIG. 4. Errors of RDMs and energy for hydrogen chains with different number of sites: (a) relative error of two-body reduced density matrix; (b) error of eigen energy for $S = 0$ and $S = 1$ states per atom. the parameters used in model calculations are from 4-site chain.

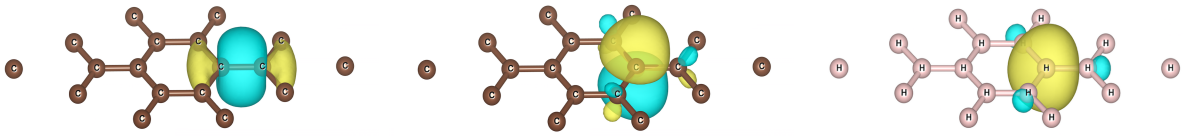

(a) (b) (c)

FIG. 5. Wannier orbitals constructed from Kohn-Sham orbitals: (a) graphene σ orbital; (b) graphene π orbitals; (c) hydrogen S orbital.

We choose a set of Slater-Jastrow wave functions corresponding to the electron-hole excitations within the π channel. The energy expectation expressed in terms of the density matrices is,

$$E = C + t(\sum_{\langle i,j\rangle,\sigma} \rho^{\sigma}_{ij} + \rho^{\sigma}_{ji}) + U \sum_{i} M^{\uparrow,\downarrow}_{ii;ii}\,, \tag{10}$$

If we have n wave functions, we can form a linear least problem of $n \times 3$ from the n constraints of Eq. (10).

$$\begin{pmatrix} E_1 \\ E_2 \\ \cdots \\ E_n \end{pmatrix} = \begin{pmatrix} 1 & \left[\sum_{\langle i,j\rangle} \rho^{\sigma}_{ij} + \rho^{\sigma}_{ji}\right]_1 & \left[\sum_i M^{\uparrow,\downarrow}_{ii;ii}\right]_1 \\ 1 & \left[\sum_{\langle i,j\rangle} \rho^{\sigma}_{ij} + \rho^{\sigma}_{ji}\right]_2 & \left[\sum_i M^{\uparrow,\downarrow}_{ii;ii}\right]_2 \\ \cdots & \cdots & \cdots \\ 1 & \left[\sum_{\langle i,j\rangle} \rho^{\sigma}_{ij} + \rho^{\sigma}_{ji}\right]_n & \left[\sum_i M^{\uparrow,\downarrow}_{ii;ii}\right]_n \end{pmatrix} \begin{pmatrix} C \\ t \\ U \end{pmatrix}. \tag{11}$$

Table II shows the final results using 25 wave functions. The errorbar is calculated using Jackniff method. Fig. 6

TABLE II. Downfolding parameters for graphene and hydrogen.

parameters [eV]	graphene	hydrogen
t	3.61(1)	3.73(1)
U	7.16(3)	9.47(5)

shows fitted energies versus the *ab initio* VMC energies. We find that the onsite Hubbard model describes graphene and hydrogen very well. The ratio of t/U is small than the semimetal-insulator transition critical value (3.8) in both the two systems, consistent to the fact that both the two systems are semimetals.

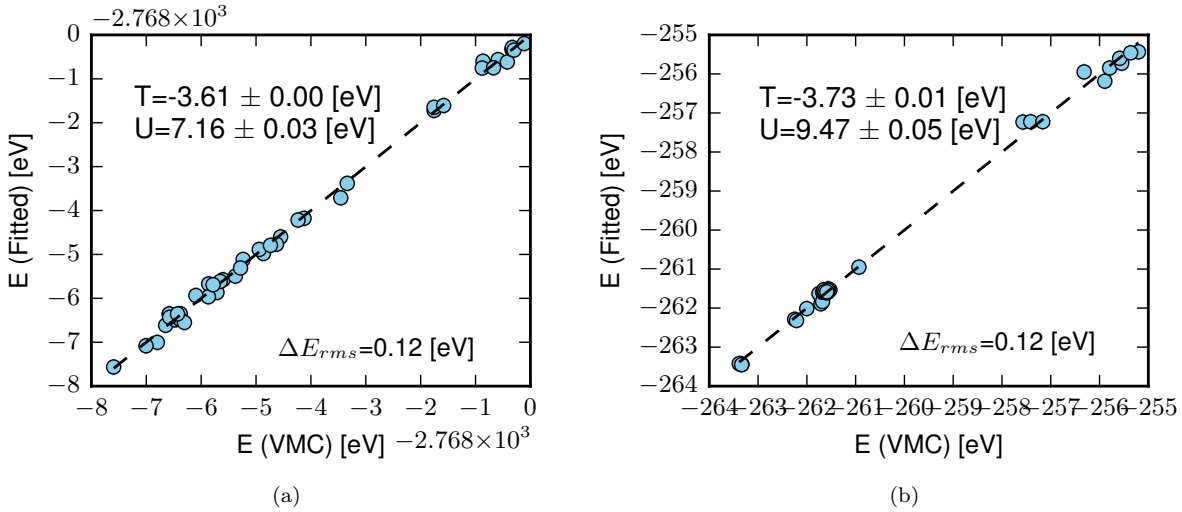

(a) (b)

FIG. 6. Comparison of *ab initio* (x-axis) and fitted energies (y-axis) of the 3×3 periodic unit cell of graphene and hydrogen lattice: (a) graphene; (b) hydrogen lattice.

IV. CONCLUSION

We have demonstrated three AIDMD methods where *ab initio* QMC data are used to fit simple effective Hamiltonians. We have elaborated on the fitting procedures. The limitations of the model are judged by assessing the quality of the fitted energies and two-body density matrices or EKT matrix elements. This feature is useful for constructing refined models needed for the accurate simulation of real materials.

This approach can be used to identify important physics degrees of freedom in complex systems for understanding macroscopic phenomena. We are at the position of applying it to more complex systems, such as transition metal oxides, high Tc cuprates.

* huihuo.zheng@anl.gov

[1] Huihuo Zheng, Yu Gan, Peter Abbamonte, and Lucas K. Wagner. The importance of sigma bonding electrons for the accurate description of electron correlation in graphene. *arXiv:1605.01076 [cond-mat]*, 2016.

[2] T. Yanagisawa. Physics of the hubbard model and high temperature superconductivity. *Journal of Physics: Conference Series*, 108(1):012010, 2008.

[3] S. Sorella, G. B. Martins, F. Becca, C. Gazza, L. Capriotti, A. Parola, and E. Dagotto. Superconductivity in the two-dimensional $\mathit{t}-\mathit{J}$ model. *Physical Review Letters*, 88(11):117002, 2002-02-28.

[4] Philip W Anderson. Twenty-five years of high-temperature superconductivity ? a personal review. *Journal of Physics: Conference Series*, 449:012001, july 2013.

[5] Steven R. White. Density matrix formulation for quantum renormalization groups. *Physical Review Letters*, 69(19):2863–2866, November 1992.

[6] Y. Nishio, N. Maeshima, A. Gendiar, and T. Nishino. Tensor Product Variational Formulation for Quantum Systems. *arXiv:cond-mat/0401115*, January 2004.

[7] G. Vidal. Class of quantum many-body states that can be efficiently simulated. *Phys. Rev. Lett.*, 101:110501, Sep 2008.

[8] F. Verstraete, V. Murg, and J.I. Cirac. Matrix product states, projected entangled pair states, and variational renormalization group methods for quantum spin systems. *Advances in Physics*, 57(2):143–224, 2008.

[9] Hitesh J. Changlani, Jesse M. Kinder, C. J. Umrigar, and Garnet Kin-Lic Chan. Approximating strongly correlated wave functions with correlator product states. *Phys. Rev. B*, 80:245116, Dec 2009.

[10] Eric Neuscamman, Hitesh Changlani, Jesse Kinder, and Garnet Kin-Lic Chan. Nonstochastic algorithms for jastrow-slater and correlator product state wave functions. *Phys. Rev. B*, 84:205132, Nov 2011.

[11] Fabio Mezzacapo, Norbert Schuch, Massimo Boninsegni, and J. Ignacio Cirac. Ground-state properties of quantum many-body systems: Entangled-plaquette states and variational monte carlo. *New J. Phys.*, 11:083026, 2009.

[12] Konrad H Marti, Bela Bauer, Markus Reiher, Matthias Troyer, and Frank Verstraete. Complete-graph tensor network states: a new fermionic wave function ansatz for molecules. *New Journal of Physics*, 12(10):103008, 2010.

[13] Gerald Knizia and Garnet Kin-Lic Chan. Density matrix embedding: A simple alternative to dynamical mean-field theory.

Phys. Rev. Lett., 109:186404, Nov 2012.
[14] Qiaoni Chen, George H. Booth, Sandeep Sharma, Gerald Knizia, and Garnet Kin-Lic Chan. Intermediate and spin-liquid phase of the half-filled honeycomb hubbard model. *Phys. Rev. B*, 89:165134, Apr 2014.
[15] Olav F. Syljuåsen and Anders W. Sandvik. Quantum monte carlo with directed loops. *Phys. Rev. E*, 66:046701, Oct 2002.
[16] R. Blankenbecler, D. J. Scalapino, and R. L. Sugar. Monte carlo calculations of coupled boson-fermion systems. i. *Phys. Rev. D*, 24:2278–2286, Oct 1981.
[17] George H Booth, Alex J W Thom, and Ali Alavi. Fermion Monte Carlo without fixed nodes: a game of life, death, and annihilation in Slater determinant space. *J. Chem. Phys.*, 131(5):054106, 2009.
[18] F. R. Petruzielo, A. A. Holmes, Hitesh J. Changlani, M. P. Nightingale, and C. J. Umrigar. Semistochastic projector monte carlo method. *Phys. Rev. Lett.*, 109:230201, Dec 2012.
[19] Eric Jeckelmann. Dynamical density-matrix renormalization-group method. *Phys. Rev. B*, 66:045114, Jul 2002.
[20] A J Daley, C Kollath, U Schollwck, and G Vidal. Time-dependent density-matrix renormalization-group using adaptive effective hilbert spaces. *Journal of Statistical Mechanics: Theory and Experiment*, 2004(04):P04005, 2004.
[21] Steven R. White and Adrian E. Feiguin. Real-time evolution using the density matrix renormalization group. *Phys. Rev. Lett.*, 93:076401, Aug 2004.
[22] E. Pavarini, I. Dasgupta, T. Saha-Dasgupta, O. Jepsen, and O. K. Andersen. Band-structure trend in hole-doped cuprates and correlation with t_{cmax}. *Phys. Rev. Lett.*, 87:047003, Jul 2001.
[23] O. K. Andersen and T. Saha-Dasgupta. Muffin-tin orbitals of arbitrary order. *Phys. Rev. B*, 62:R16219–R16222, Dec 2000.
[24] F. Aryasetiawan, M. Imada, A. Georges, G. Kotliar, S. Biermann, and A. I. Lichtenstein. Frequency-dependent local interactions and low-energy effective models from electronic structure calculations. *Phys. Rev. B*, 70:195104, Nov 2004.
[25] Harald O. Jeschke, Francesc Salvat-Pujol, and Roser Valentí. First-principles determination of heisenberg hamiltonian parameters for the spin-$\frac{1}{2}$ kagome antiferromagnet $\mathrm{zncu_3(oh)_6cl_2}$. *Phys. Rev. B*, 88:075106, Aug 2013.
[26] N. S. Fedorova, C. Ederer, N. A. Spaldin, A. Scaramucci, arXiv:1412.3702.
[27] Lucas K. Wagner and Peter Abbamonte. Effect of electron correlation on the electronic structure and spin-lattice coupling of high-tc cuprates: Quantum monte carlo calculations. *Physical Review B*, 90(12):125129, September 2014.
[28] Karl F. Freed. Is there a bridge between ab initio and semiempirical theories of valence? *Accounts of Chemical Research*, 16(4):137–144, 1983.
[29] S. Q. Zhou and D. M. Ceperley. Construction of localized wave functions for a disordered optical lattice and analysis of the resulting hubbard model parameters. *Phys. Rev. A*, 81:013402, Jan 2010.
[30] Seiichiro Ten-no. Stochastic determination of effective hamiltonian for the full configuration interaction solution of quasi-degenerate electronic states. *The Journal of Chemical Physics*, 138(16):–, 2013.
[31] Stanisław D. Głazek and Kenneth G. Wilson. Renormalization of hamiltonians. *Phys. Rev. D*, 48:5863–5872, Dec 1993.
[32] Franz Wegner. Flow-equations for hamiltonians. *Annalen der Physik*, 506(2):77–91, 1994.
[33] Steven R. White. Numerical canonical transformation approach to quantum many-body problems. *The Journal of Chemical Physics*, 117(16):7472–7482, 2002.
[34] Takeshi Yanai and Garnet Kin-Lic Chan. Canonical transformation theory for multireference problems. *The Journal of Chemical Physics*, 124(19):–, 2006.
[35] T. J. Watson Jr., G. K-L Chan, arXiv:1502.04698.
[36] Motoaki Hirayama, Takashi Miyake, and Masatoshi Imada. Derivation of static low-energy effective models by an *ab initio* downfolding method without double counting of coulomb correlations: Application to $\mathrm{srvo_3}$, fese, and fete. *Phys. Rev. B*, 87:195144, May 2013.
[37] Kazuma Nakamura, Yoshihide Yoshimoto, Yoshiro Nohara, and Masatoshi Imada. Ab initio low-dimensional physics opened up by dimensional downfolding: Application to lafeaso. *Journal of the Physical Society of Japan*, 79(12):123708, 2010.
[38] F. Nilsson, R. Sakuma, and F. Aryasetiawan. *Ab initio* calculations of the hubbard u for the early lanthanides using the constrained random-phase approximation. *Phys. Rev. B*, 88:125123, Sep 2013.
[39] F. Aryasetiawan, K. Karlsson, O. Jepsen, and U. Schönberger. Calculations of hubbard u from first-principles. *Phys. Rev. B*, 74:125106, Sep 2006.
[40] E. P. Scriven and B. J. Powell. Geometrical frustration in the spin liquid $\beta^{'}\mathrm{m_3etsb[pd(dmit)_2]_2}$ and the valence-bond solid $Me_3etp[pd(dmit)_2]_2$. *Phys. Rev. Lett.*, 109:097206, Aug 2012.
[41] T. O. Wehling, E. Sasioglu, C. Friedrich, A. I. Lichtenstein, M. I. Katsnelson, and S. Blügel. Strength of effective coulomb interactions in graphene and graphite. *Physical Review Letters*, 106(23):236805, June 2011.
[42] Hiroshi Shinaoka, Rei Sakuma, Philipp Werner, Matthias Troyer, arXiv:1410.1276.